NURETH14-055

BOILING HEAT TRANSFER IN POROUS MEDIA COMPOSED OF PARTICLES

Bofeng Bai¹, Xiaojie Zhang ^{1,2}, Ke Wang¹

¹ State Key Laboratory of Multiphase Flow in Power Engineering, Xi'an Jiaotong University, China
² State Nuclear Power Engineering Company, Shanghai, China
bfbai@mail.xjtu.edu.cn, xiaojie_zh@hotmail.com, justin0521@163.com

Abstract

The boiling heat transfer in the porous media composed of spherical fuel elements exerts significant influences on the reactor's efficiency and safety. In the present study an experimental setup was designed and the boiling heat transfer in the porous media composed of spheres of regular distribution was investigated. Four spheres with diameters of 5mm, 6mm, 7mm and 8mm were used in the test sections. The greater particle diameter led to lower heat transfer coefficient, and resulted in higher wall superheat of original nucleation boiling. The variation of heat transfer coefficient was divided into three groups according to two-phase flow patterns and void fraction. A correlation of heat transfer coefficient was proposed with a mean relative deviation of \pm 16%.

1. Introduction

The spherical fuel element nuclear reactor shows great promise because of its advantages in safety, fuel utilization, small volume and economy [[1]~[4]]. In the core of the reactor, it is porous media composed of small spherical fuel elements which serve as the heating source of the coolant. The boiling heat transfer exerts significant influences on the reactor. However, the study on the reactor's thermal-hydraulic is still in its infancy and the relevant cognition is not profound enough. Also there are some different or even conflicting conclusions because of the complexity and speciality of the porous structure composed of particles and the difficulty in the experimental simulation [[5]].

According to Jiang Pei-Xue' [[6]] [[7]] and M. Jamialahmadi's [[8]] researches, the heat transfer increases with the increase of the particle diameter, but the conclusion is contrary to Jeigranik's and Hwang's [[10]] researches. There are few published experimental researches about the heat transfer of porous media which serve as the heating source. Such studies are of great significance, because in pebble bed reactors the spherical fuel elements serve as the heating source. Naik and Dhir [[10]] concluded the temperature distribution along the direction of flow for water flowing through layers of inductively heated steel particles, but in the experiment, the heating by the particles is non-uniform because of the skin effect [[10]~[13]]. Therefore, the uniform heating of the fluid by the particles is one of key to the experiment. Most researches are qualitative [14,15,16] and quantitative researches are very few.

In the present research, an experimental simulation is proposed to obtain the pertinent data on boiling heat transfer parameters in porous media composed of heating particles. The effects of particle diameter, heat flux and mass flux on the boiling heat transfer are investigated, respectively, and a correlation of heat transfer coefficient is concluded.

2. Experimental techniques

2.1 Experimental Apparatus

The apparatus for the measurement of the heat transfer in channels packed with particles is shown in Figure 1. Its major parts include a test section, a temperature controller, a preheater, a flowmeter, a liquid vessel and a condenser. The deionized water pumped from the liquid vessel and flowing through the filter and the flowmeter is heated to the desired temperature in the preheater by an electrically resistant heater which is controlled by the temperature controller. The fluid flows through the test section, the condenser and finally goes back into the liquid vessel.

The test section, as is shown in Figure 2, is purposefully designed for both the heating of the particles and the visual observation of the two-phase flow pattern. It consists of a polycarbonate plate on one side for the observation, an irregular aluminum structure with densely distributed hemispheres on the other side as the heating source of the fluid, which is shown in Figure 3. There is a layer of glass particles between the polycarbonate plate and the aluminum plate for the improvement of the flow uniformity perpendicular to the flow direction. The diameters of the hemispheres on the irregular aluminum structure and of the glass particles are the same. The electrically resistant heater is for the heating of the irregular aluminum structure, the mica for the insulation, the asbestos for the prevention of the heat loss of the test section and the metal plate for fastening. Four different types of packing composed of particles are employed, the specifications of which are shown in Table 1. The experimental parameters including particle diameter d_p , fluid inlet temperature T_{in} , vapor quality x, Re number and heat flux q are shown in Table 2.

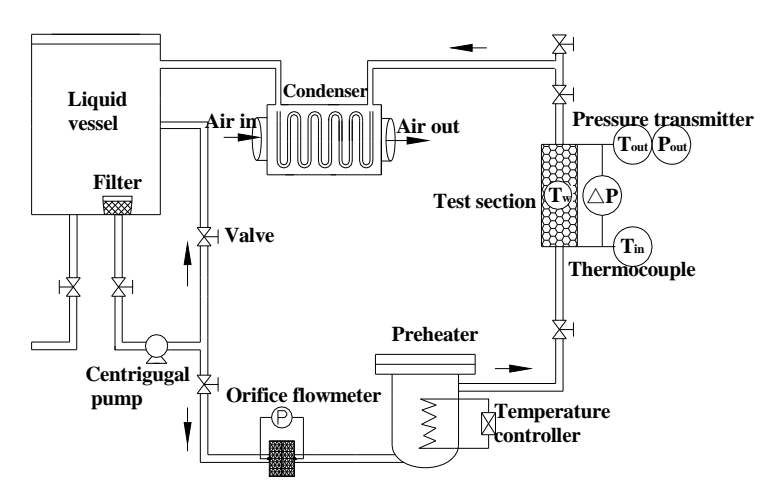


Figure 1 Experimental apparatus

2.2 Uncertainty Analysis and Data Reduction

Six K-type thermocouples with the uncertainty of $\pm 0.1\,^{\circ}$ C are used to measure the temperature of the irregular aluminum structure, as is shown in Figur 4. The thermocouples are fixed on the bottom of the holes, which are in the backside of the aluminum structure. Thermocouples 1 and thermocouple 2 are for the measurement of the pore temperature, and thermocouples 3, 4, 5 and 6 for the measurement of the particle temperature. Two T-type thermocouples are employed to measure the inlet and outlet fluid temperature with the uncertainty of $\pm 0.1\,^{\circ}$ C. The water flow is measured by an orifice mass flux meter with the uncertainty of 0.5%, the outlet pressure of the test section by a

The 14th International Topical Meeting on Nuclear Reactor Thermalhydraulics, NURETH-14 Toronto, Ontario, Canada, September 25-30, 2011

static pressure transmitter with the uncertainty of $\pm 0.1\%$, and the pressure drop by a Rosemount 3051 transmitter with the uncertainty of $\pm 0.5\%$. An AC voltage transmitter and a current transmitter are employed for the measurement of the heating voltage and current of the test section with the uncertainty of $\pm 0.2\%$.

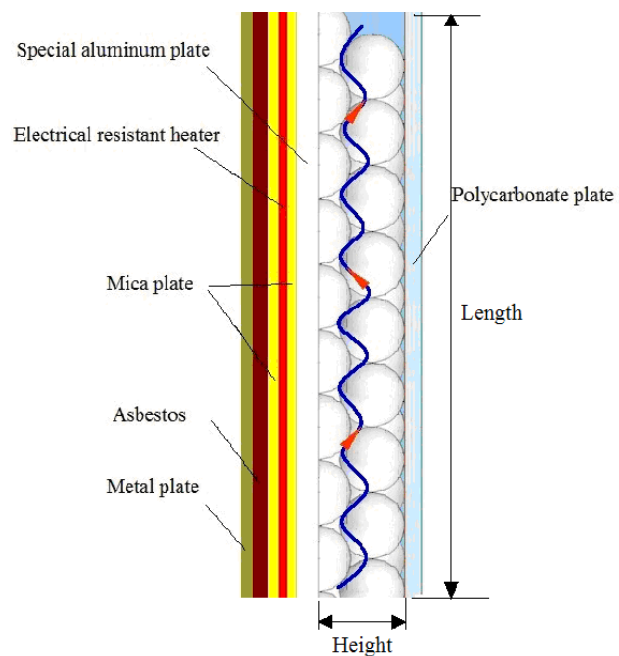


Figure 2 Test section



Figure 3 Irregular aluminum structure

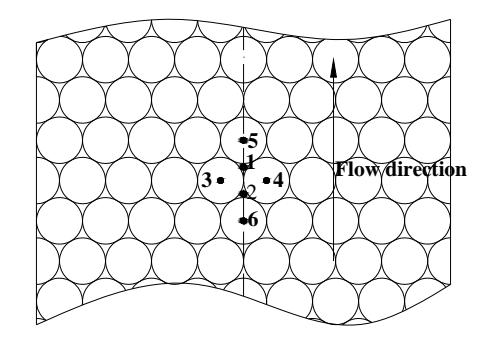


Figure 4 Positions of thermocouples on irregular aluminum structure

Table 1 Specifications of the test section

Case No.	1	2	3	4
Particle diameter $d_p(mm)$	5	6	7	8
Length(mm)	260.48	311.80	364.67	361.33
Width(mm)	45	54	63	72
Height(mm)	6.58	7.9	9.22	10.53
Porosity	0.3667	0.3780	0.3883	0.3976

Table 2 Experimental parameters

$d_p(\mathbf{mm})$	$T_{in}(^{\circ}\mathbb{C})$	Vapour quality	Re		$q(\mathbf{kW \cdot m^{-2}})$	
		x_{max}	min	max	min	max
5	80	0.16	466	4897	2.6	287.1
6	80	0.21	289	4862	0.8	329.8
7	80	0.16	330	3987	0.2	164.0
8	80	0.10	464	4744	0.2	123.4

The inlet pressure is calculated by

$$p_{in} = p_{out} + \Delta p \tag{1}$$

The 14th International Topical Meeting on Nuclear Reactor Thermalhydraulics, NURETH-14 Toronto, Ontario, Canada, September 25-30, 2011

The fluid pressure p_f at the measured cross section is calculated in terms of the inlet pressure and the pressure drop,

$$p_f = p_{in} - \Delta p L_{in-c} / L \tag{2}$$

where L_{in-c} is the distance between the inlet and the measured cross section, and L is the distance between the inlet and the outlet.

The heating efficiency of the test section ξ is determined according to the actual heating power and the fluid enthalpy difference between the inlet and the outlet under single-phase flow,

$$\xi = \frac{GA_{channel} \left(h_{out} - h_{in} \right)}{I/I} \tag{3}$$

where G is the fluid mass flux, $A_{channel}$ is the area of the cross section, h_{in} and h_{out} are the liquid enthalpy at the inlet and the outlet respectively, U is the voltage across the resistant heater, and I is the current through the resistant heater.

The heat flux q is determined by

$$q = \xi UI/A \tag{4}$$

where A is the heating area of the irregular aluminum structure.

In two-phase flow, the specific enthalpy on the saturated vapor line $h_{y,sat}$ at any cross section y is calculated according to the pressure of the fluid. The critical cross section of the original saturated boiling, y_{cr} , is determined by

$$h_{ycr,sat} = h_{in} + \frac{\xi UIL_{ycr}}{GA_{channel}L} \tag{5}$$

It is single-phase or sub-cooled boiling before y_{cr} , and saturated boiling after y_{cr} . In single-phase flow or sub-cooled boiling, the bulk fluid temperature is determined by

$$T_f = T_{in} + \left(T_{ycr,sat} - T_{in}\right) L_{in-c} / L_{ycr} \tag{6}$$

In saturated boiling, the bulk fluid temperature equals the saturation temperature,

$$T_f = T_{c sat} \tag{7}$$

Figure 5 shows a typical arrangement of seven adjacent particles. Each particle is in the proximity of six other particles and each pore is in the proximity of three particles. Therefore, one sixth of a particle and one third of a pore can be treated as constitute a unit. The data reduction about the wall temperature of the irregular aluminum structure is based on the unit.

Wall temperature, T_{wi} ($i=1\sim4$), are determined by the measured temperature; T_i ($i=1\sim4$), and heat conduction equation,

$$q = K \left(T_i - T_{wi} \right) / \Delta x_i \tag{8}$$

The 14th International Topical Meeting on Nuclear Reactor Thermalhydraulics, NURETH-14 Toronto, Ontario, Canada, September 25-30, 2011

where K is the thermal conductivity of the aluminum structure, and Δx_i ($i=1\sim4$) are the distances between the thermocouples 1 and 4 and equal to 2mm in the present experiment.

The geometric position of the wall temperature is shown in Figure 6. In the temperature unit composed of S_2 and S_3 , the following relationship is obtained according to the law of heat transfer,

$$a(\overline{T}_{w,2-3} - T_f)(S_3 + S_2) = a_3(\overline{T}_{w3} - T_f)S_3 + a_2(T_{w2} - T_f)S_2$$
(9)

$$\overline{T}_{w3}S_3 = \frac{1}{6} \iint \frac{R}{\sqrt{R^2 - x^2 - y^2}} \left[T_2 - \frac{(T_2 - T_3)\sqrt{R^2 - x^2 - y^2}}{R} \right] dxdy \tag{10}$$

It is supposed that the heat transfer coefficients are equal, that is

$$a = a_3 = a_2 \tag{11}$$

$$\overline{T}_{w,2-3} = T_f + \frac{\frac{1}{6} \iint \frac{R}{\sqrt{R^2 - x^2 - y^2}} \left[T_2 - \frac{(T_2 - T_3)\sqrt{R^2 - x^2 - y^2}}{R} \right] dx dy - T_f S_3 + (T_{w2} - T_f) S_2}{S_2 + S_3}$$
(12)

 $\bar{T}_{w,2-4}$, $\bar{T}_{w,1-3}$, and $\bar{T}_{w,1-4}$ are calculated in the same way, and the average temperature of the surface of the irregular aluminum structure is calculated by

$$\overline{T}_{w} = \left(\overline{T}_{w,1-3} + \overline{T}_{w,1-4} + \overline{T}_{w,2-3} + \overline{T}_{w,2-4}\right)/4 \tag{13}$$

The heat transfer of the porous media composed of particles is determined as follows



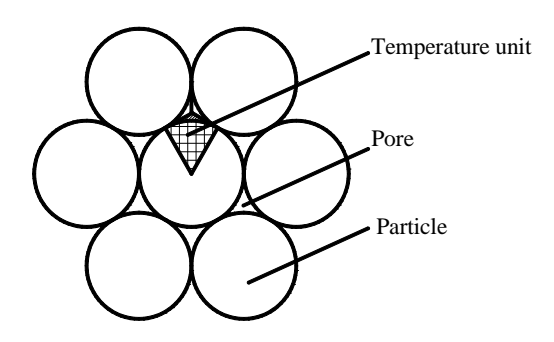


Figure 5 Typical arrangement of adjacent particles

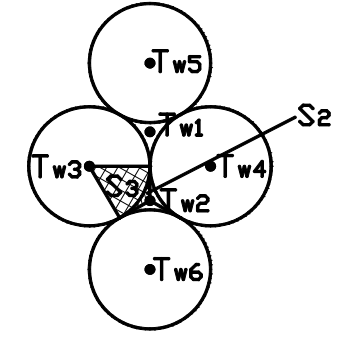


Figure 6 Geometric position of wall temperature

In saturated boiling the vapor quality x is determined by

$$x = (h - h_f) / h_{fg} \tag{15}$$

where h is the total enthalpy of the two-phase mixtures, h_f the enthalpy of the saturated liquid and h_{fg} is the latent heat of evaporation.

In sub-cooled boiling, the vapor quality is determined by Bowring law (1962):

$$x = e(h - h_D) / h_{fg} \tag{16}$$

where e is the fraction of the heat which is used for the liquid evaporation. The h_D is the fluid enthalpy at the departure point of the bubbles.

The void fraction is determined by the correlation of Maien/Coddington [17].

3. Experimental results

3.1 Boiling curves

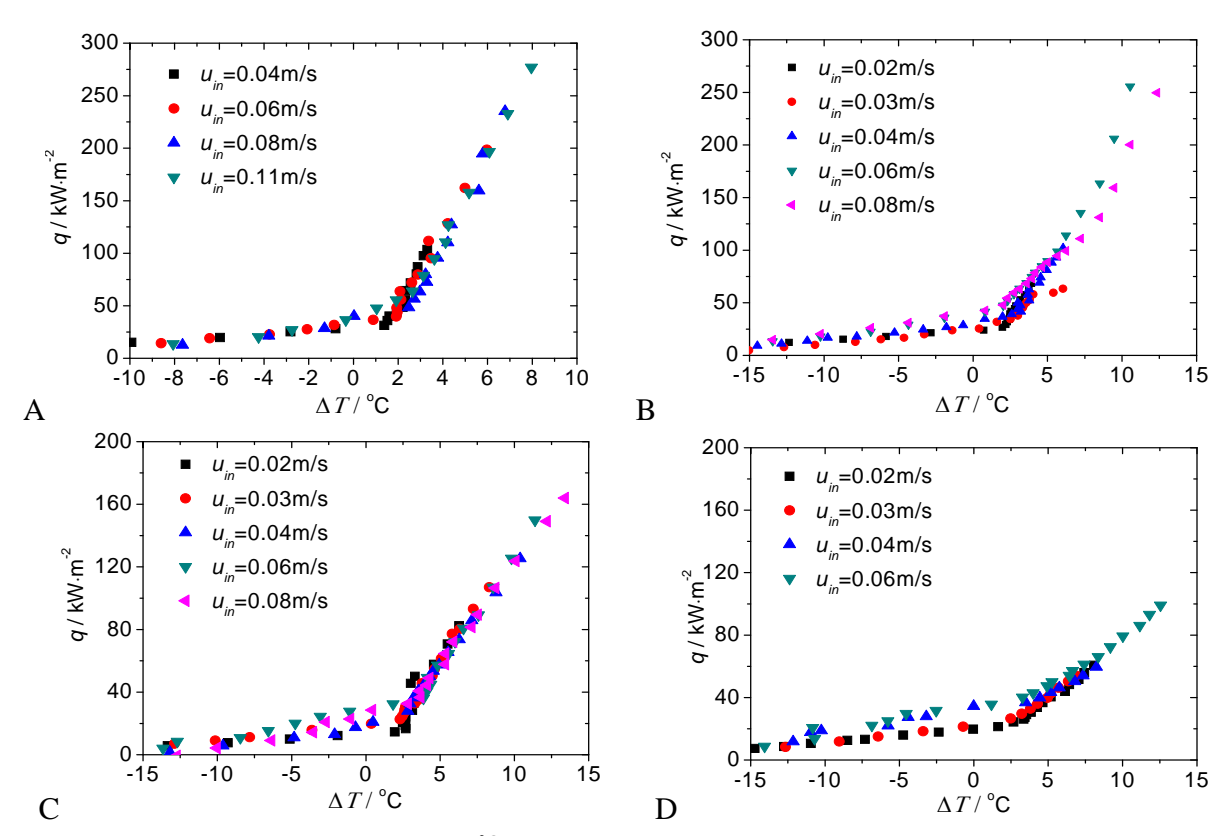


Figure 7 Boiling curves ($T_{in}=80^{\circ}C$). (A) $d_p=5$ mm, (B) $d_p=6$ mm, (C) $d_p=7$ mm, (D) $d_p=8$ mm

When boiling occurs in the porous channel, a characteristic boiling curve can be presented in terms of the wall superheats versus the heat flux at the wall. Figure 7 (A), (B), (C) and (D) show the boiling curves for the porous channels composed of particles with diameters of 5mm, 6mm, 7mm and 8mm, respectively. In single-phase flow region, the heat transfer coefficient is low and approximately linearly related to the wall superheats. The heat transfer coefficient increases dramatically in two-phase flow region. As is shown, boiling occurs with low superheats at the wall. Moreover, the wall superheats of the original nucleation boiling increase with the increase of the particle diameter. It indicates that the increase of the particle diameter deteriorates the heat transfer.

3.2 Effect of void fraction

Figure 8 (A), (B), (C) and (D) show the heat transfer coefficients versus the void fractions for the porous channels composed of particles with diameters of 5mm, 6mm, 7mm and 8mm, respectively. The variation of heat transfer coefficients can be divided into three areas according to two-phase flow patterns and void fraction: low void fraction area, high void fraction area and middle void fraction area. It is bubbly flow in low void fraction area and boiling heat transfer coefficient increases rapidly with the increase of void fraction. It is annular flow in high void fraction area, and heat transfer coefficient increases dramatically with the increase of void fraction. However, heat transfer coefficient increases slowly in middle void fraction area, in which slug flow occurs.

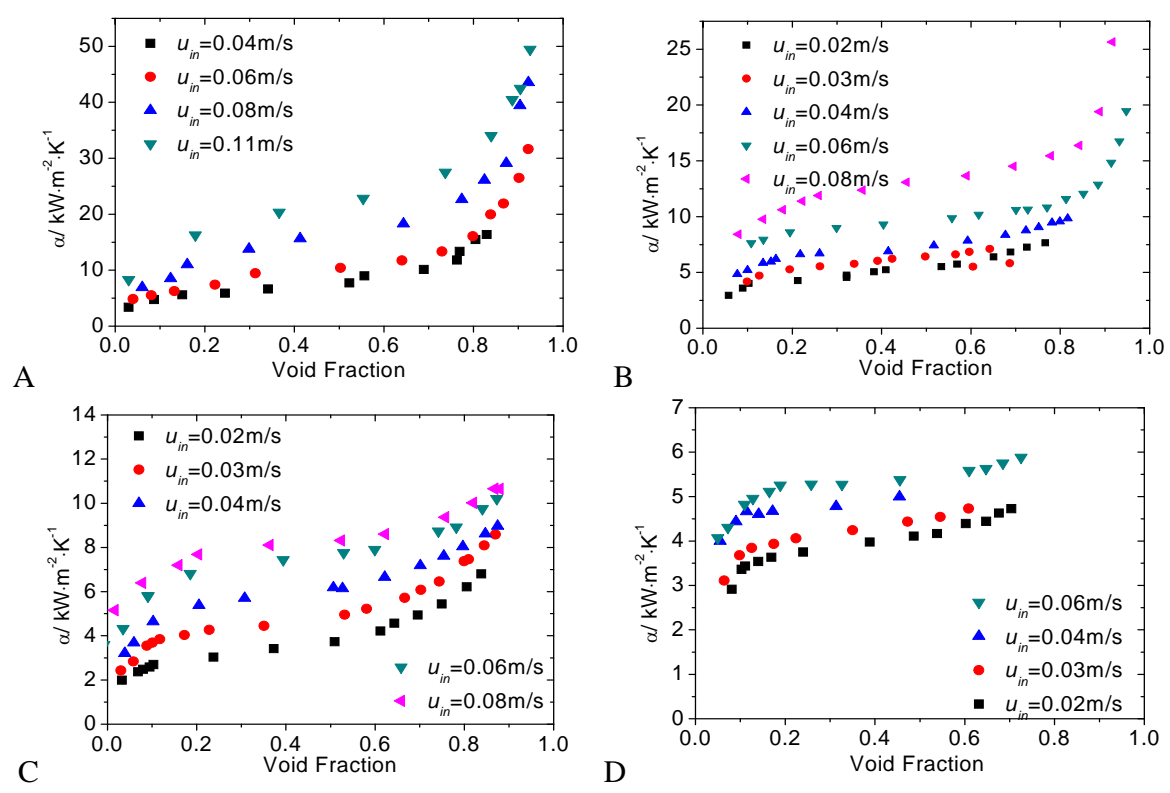


Figure 8 Effect of void fraction on heat transfer coefficient (Tin=80°C). (A) d_p =5mm, (B) d_p =6mm, (C) d_p =7mm, (D) d_p =8mm

3.3 Effect of heat flux

Figure 9 (a), (b), (c), (d) show the heat transfer coefficients versus heat flux for porous channels composed of particles with diameters of 5mm, 6mm, 7mm, 8mm, respectively. The effect of heat flux on heat transfer coefficient is significant. The boiling is more intense at higher heat flux, leading to the increase of the heat transfer. Therefore, heat transfer coefficient increases with the increase of heat flux.

3.4 Effect of mass flux

Figure 9 (a), (b), (c), (d) also show the heat transfer coefficients at different mass flux of porous channels composed of particles with diameters of 5mm, 6mm, 7mm, 8mm, respectively. The flow disturbance is more intense with the increase of mass flux, which leads to the increase of the heat transfer coefficient. Consequently, heat transfer coefficient increases with the increase of mass flux.

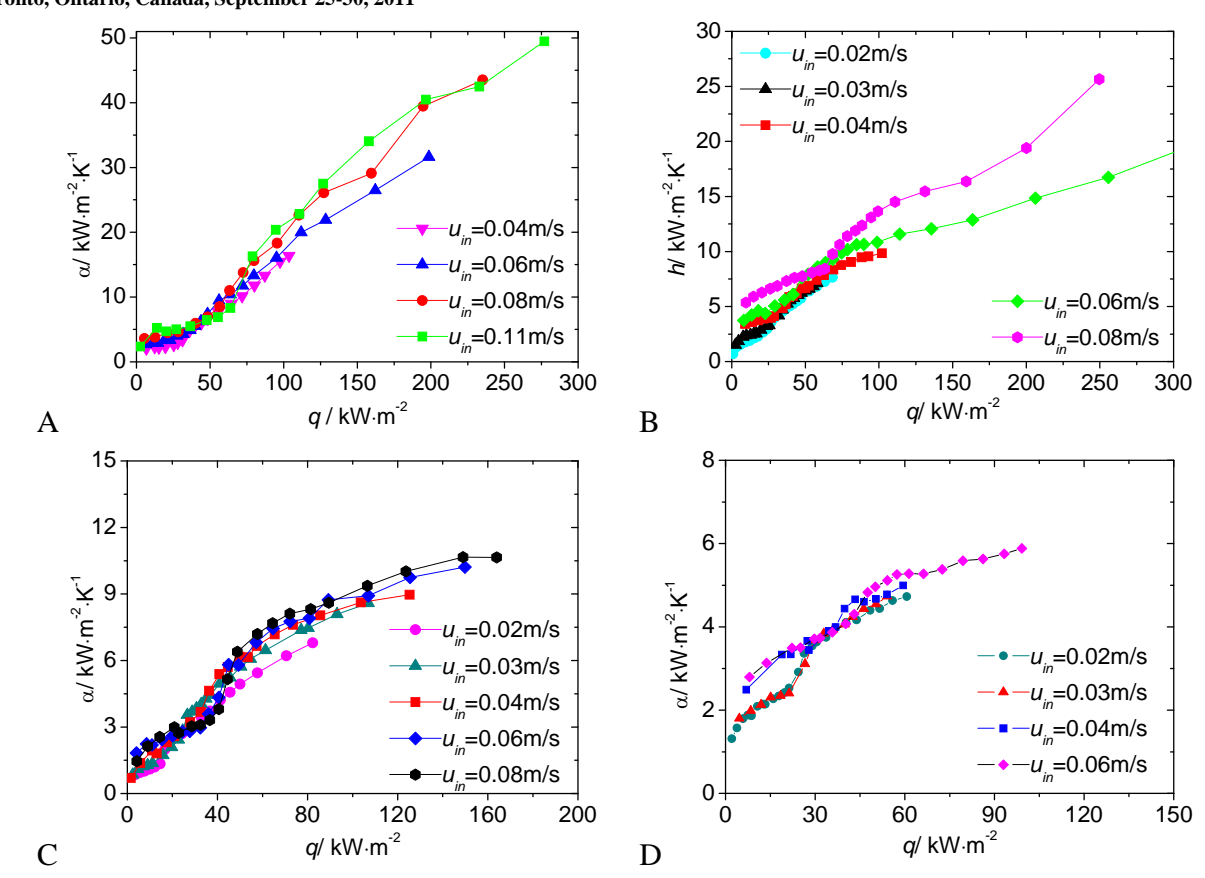


Figure 9 Effect of mass flux on heat transfer coefficient (Tin=80°C). (A) d_p =5mm, (B) d_p =6mm, (C) d_p =7mm, (D) d_p =8mm

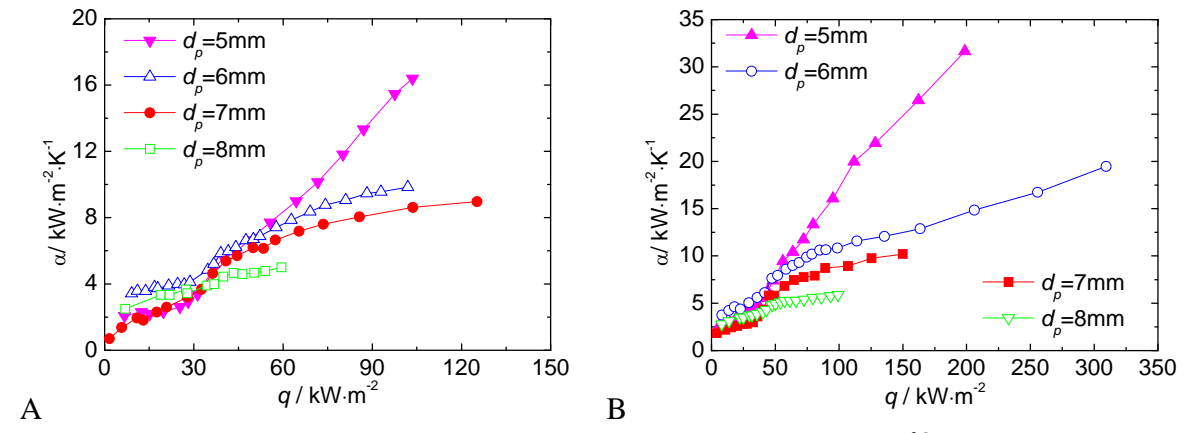


Figure 10 Effect of particle diameter on heat transfer coefficient (Tin=80°C). (A) u_{in} =0.04 m/s, (B) u_{in} =0.06 m/s

3.5 Effect of particle diameter

Figure 10 (a) and (b) show the heat transfer coefficients at different particle diameters. The greater particle diameter leads to lower heat transfer coefficient. The smaller the particle diameter is, the smaller the pore is and the more intense the disturbances of fluid flow are, the more frequently the

bubbles split and merge. These all lead to the increase of heat transfer. Consequently, boiling heat transfer coefficient increases with the decrease of particle diameter.

3.6 Correlation of boiling heat transfer coefficient

In the present research, the porosity and the dimensionless parameter Bo are employed in order to take the effects of particle diameter and heat flux into account. Thus, the heat transfer in porous media composed of particles is related to Re, Pr, Bo and ε , and the experimental results can be correlated by the following equations:

$$Nu = a \cdot \varepsilon^{-b} \cdot Bo^{c} \cdot Re_{l}^{d} \cdot Pr_{l}^{e}$$
(17)

$$Nu = \frac{\alpha d_p}{\lambda}, \quad Bo = \frac{q}{Gh_{fg}}, \quad Re_l = \frac{\rho_l J_l d_p}{\eta_l} = \frac{G(1-x)d_p}{\eta_l}, \quad Pr_l = \frac{\upsilon_l}{a_l}$$
(18)

where a, b, c, d, e are constants. λ is the thermal conductivity of the fluid, ρ_l the density of the liquid, J_l the superficial velocity of the liquid, η_l the dynamic viscosity of the liquid, v_l the kinematic viscosity of the liquid and a_l is the thermal diffusivity of the liquid.

In the present experiment, a=0.447, b=0.425, c=0.741, d=0.697, e=0.33. The mean relative deviation of the correlation is $\pm 16\%$ as is shown in Figure 11.

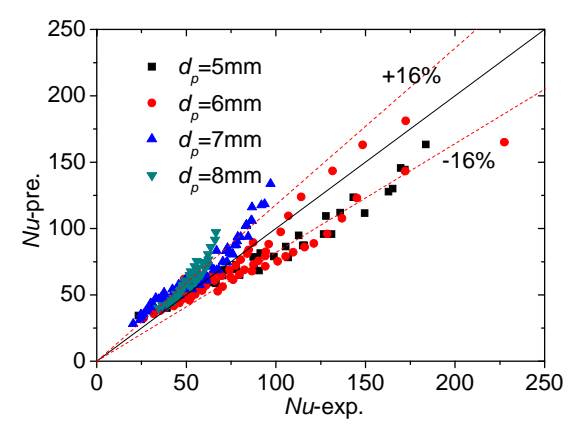


Figure 11 Comparison of current model with present experimental data

4. Conclusions

This paper presents an experimental simulation for the study of boiling heat transfer through porous media composed of heating particles. A correlation is proposed to calculate the boiling heat transfer coefficient from the experiments. The boiling heat transfer in porous media is affected by heat flux, mass flux, and particle diameter. Heat transfer coefficient increases with the increase of heat flux and mass flux. The greater particle diameter leads to a lower heat transfer coefficient, and results in a higher wall superheat of original nucleation boiling. The variation of heat transfer coefficient can be divided into three areas according to flow patterns and void fraction: low void fraction area, high void fraction area and middle void fraction area. An empirical correlation of Nu is presented in form of $Nu = a \cdot \varepsilon^{-b} \cdot Bo^c \cdot Re_l^d \cdot Pr_l^e$, and a = 0.447, b = 0.425, c = 0.741, d = 0.697, e = 0.33, with mean relative deviation of $\pm 16\%$.

5. References

- [1] C. Kadak, "A future for nuclear energy: pebble bed reactors", Int. J. Critical Infrastructures, Vol. 1, 2005, pp.330-345.
- [2] V. T. Georgi, E. S. Thomas, E. W. Alan, et al., "Long Life Small Nuclear Reactor Without Open-Vessel Re-Fueling", Pacific Northwest National Laboratory, 2005.
- [3] F. Sefidvash, "Preliminary evaluation of the fixed and fluidized bed nuclear reactor concept using the IAEA-INPRO methodology", Car Haser Verlag, Nunchen, 2004.
- [4] "Fixed Bed Nuclear Reactor (FBNR)", University of Rio Grande do Sul, 2006.
- [5] X. Yan, Z. J. Xiao, Y. P. Huang, et al., "Research progress on flow and heat transfer in porous media", Nuclear Power Fngineering, Vol. 27, 2006, pp.77-82.
- [6] P. X. Jiang, M. Li, etal, "Experimental Research on Convection heat Transfer in Sintered Porous Plate Channels", Int. J. Heat and Mass Transfer, Vol. 47, 2004, pp.2085-2096.
- [7] P. X. Jiang, Z. Wang, Z. P. Ren, et al, "Experimental Research of Fluid Flow and Convection Heat Transfer in Plate Channels Filled with Glass or Metallic Particles", Experimental Thermal and Fluid Science, Vol. 20, 1999, pp.45-54.
- [8] M. Jamialahmadi, H. Muller-Steinhagen, M. R. Izadpanah, "Pressure drop, gas hold-up and heat transfer during single and two-phase flow through porous media", Int. J. Heat and Fluid Flow, Vol. 26, 2005, pp.156-172.
- [9] U. A. Jeigarnik, F. P. Ivanov, N. P. Ikranikov, "Experimental Data on Heat Transfer and Hydraulic Resistance in Unregulated Porous Structures", Teploenergetika, Vol. 21, 1991, pp.33-38.
- [10] G. J. Hwang, C. H. Chao, "Heat transfer measurement and analysis for sintered porous channels", J. Heat Transfer, Vol. 116, 1994, pp.456-464.
- [11] A. S. Naik, V. K. Dhir, "Forced Flow Evaporative Cooling of a Volumetrically Heated Porous Layer", Int. J. Heat and Mass Transfer, Vol. 25, 1982, pp.541-552.
- [12]P. Schafer, "Boiling experiments for the validation of dryout models used in reactor safety", Nuclear Engineering and Design, Vol. 236, 2006, pp.1511-1519.
- [13] K. Atkhen, G. Berthoud, "SILFIDE experiment: Coolability in a volumetrically heated debris bed", Nuclear Engineering and Design, Vol. 236, 2006, pp.2126-2134.
- [14] Q. Liao, T. S. Zhao, "A visual study of phase-change heat transfer in a two-dimensional porous structure with a partial heating boundary", Int. J. Heat and Mass Transfer, Vol. 43, 2000, pp.1089-1102.
- [15]Z. Q. Chen, P. Cheng, T. S. Zhao, "An Experimental Study of Two Phase Flow and Boiling Heat Transfer in Bi-Dispersed Porous Channels", Int. Comm. Heat Mass Transfer, Vol. 27, 2000, pp.293-302.
- [16] X. L. Cao, "An experimental study on evaporative heat transfer in bi-dispersed wick structures", Journal of Astronautics, Vol. 25, 2004, pp.690-692.

The $14^{\rm th}$ International Topical Meeting on Nuclear Reactor Thermalhydraulics, NURETH-14 Toronto, Ontario, Canada, September 25-30, 2011

[17]P. Coddington, R. Marican, "A study of the performance of void fraction correlations used in the context of drift-flux two-phase flow models", Nuclear Engineering and Design, Vol. 215, 2002, pp.199-216.